

## **A NEW ENERGY MANAGEMENT SYSTEM OF ON-GRID / OFF-GRID USING ADAPTIVE NEURO-FUZZY INFERENCE SYSTEM**

BILAL NAJI ALHASNAWI<sup>1,\*</sup>, BASIL H. JASIM<sup>2</sup>

<sup>1</sup>Collage of Engineering, Electrical Engineering Department,  
University of Basrah, 61001, Basrah, Iraq

<sup>2</sup>Collage of Engineering, Electrical Engineering Department,  
University of Basrah, 61001, Basrah, Iraq

\*Corresponding Author: bilalnaji11@yahoo.com

### **Abstract**

This paper proposed a novel energy management system for grid-connected mode and islanded mode. In this paper, a hybrid system that includes distribution electric grid, photovoltaic, and batteries are employed as energy sources in the residential of the consumer in order to meet the demand. The proposed system permits coordinated operation of distributed energy resources to concede necessary active power and additional service whenever required. This paper uses a home energy management system which switches between the distributed energy and the grid power sources. The home energy management system incorporates controllers for maximum power point tracking, battery charge and discharge, and inverter for effective control between different sources depending upon load requirement and availability of sources at the maximum power point. Also, this paper aims to demonstrate the usefulness of the adaptive neuro-fuzzy inference system for tracking maximum power in a photovoltaic system. The simulation results have verified the effectiveness and feasibility of the introduced strategy and the capability of proposed controller for a hybrid microgrid operating in different modes. The results showed that 1) energy management and energy interchange were effective and contributed to cost reductions, CO<sub>2</sub> mitigation, and reduction of primary energy consumption and 2) the developed new energy management system proved to provide more robust and high performance control than conventional energy management systems. Also, the results demonstrate the effectiveness of the proposed robust model for the microgrid energy management.

Keywords: Adaptive neuro-fuzzy inference system (ANFIS), Energy management system, Hybrid renewable energy.

## 1. Introduction

Microgrids are low-voltage small-scale electrical networks composed of distributed energy resources, such as energy storage systems, distributed generation systems, and controllable and non-controllable loads. This set of technologies requires a management system capable of controlling, supervising, and planning its operation while guaranteeing a reliable performance, economical, and efficient. Currently, with the evolution of new digital technologies, such as micro-processed systems, and advances in power electronics, many applications have been implemented in the smart grid, specifically in the development of controllers and electronic energy converters. In recent years, researchers have made significant contributions that have a high impact in these areas, mainly aimed at data acquisition, automation, and control of microgrids [1]. The microgrids not only integrate the distributed generation to the utility grid in a reliable and clean fashion but also provide high reliability in its capacity to operate in the face of natural phenomena and active distribution grids, which in turn results in less energy losses in transmission and distribution and less construction and investment time [2]

Since the management functionalities of a microgrid deal with issues from different technical areas, timescales, and infrastructure levels, the hierarchical control scheme has been widely accepted as a standardized solution. The adoption of a hierarchical control scheme becomes more relevant when it is used to analyse different processing times required to execute the main processes at each control level: first, fast dynamic control of voltages and frequency of the DER units is used to maintain the system's stability; second, slower dynamic control is deployed for the long-term economic dispatch. The idea behind these different control levels is that each level operates with its own processing time, data inputs, and infrastructure requirements. In general, the hierarchical control comprises three levels: (1) primary level, responsible for local control of the distributed energy resources, (2) secondary level, which deals with primary deviations in variables as voltage and frequency, (3) tertiary level, which is also known as the energy management system, which introduces smart to the system to coordinate and manage the operation of optimal power flows [3-11].

The rest of this paper is organized as follows. Section 2 describes the related work. Section 3 presents a description of the proposed system. Section 4 presents the ANFIS system, Section 5 presents maximum power point methods, Section 6 presents the ANFIS method based on MPPT. Section 7 presents the home energy management system. Section 8 presents the results of the proposed method, Finally, Section 9 concludes the paper.

## 2. Related Works

In this section, we review relevant research covering energy management strategies in the context of areas related to this work. In Gules et al. [12] research, the photovoltaic system with batteries backup is operated in the islanded and grid-connected modes of operation. In this paper, separate control algorithms are implemented for Inverter, Battery, and photovoltaic array for maximum utilization of available sources for meeting the energy requirement of the consumer. Kalika et al. [13] presented a neural fuzzy controller based maximum power point. The neural network is used to compute MPPT voltage depended on given irradiation and temperature values, while the fuzzy logic controller is used to force the photovoltaic

panel voltage to track MPTT voltage by changing of the duty ratio of the buck-boost converter. The simulation result reveals that the neural-fuzzy controller track MPPT effectively under rapid variation of load, irradiation, and temperature.

Kharb et al. [14] presented the design and implementation of the Adaptive Neuro-Fuzzy Inference System (ANFIS) based MPPT. The MPPT controller is composed of ANFIS and PI controller. The result of the simulation shows that the ANFIS controller can track the maximum power point effectively and quickly under varying the atmospheric conditions. Specially, under little irradiation, the proposed controller can track MPPT without high oscillations of the power and during short response time. In [15], Mahdavi et al. proposed ANFIS based maximum power point controller. The proposed controller is composed of FLC and ANFIS. The ANFIS works as a reference model of the photovoltaic module and computes maximum power point voltage ( $V_{mpp}$ ) from input variables of the ANFIS which are temperature and irradiation. While the input of the FLC is the error that is computed by the difference between  $V_{mpp}$  and output voltage of the photovoltaic module; and output of the fuzzy logic controller is fed to a duty cycle of the buck-boost converter. The simulation results reveal that the ANFIS controller is less oscillation and fast response than the FLC. In [16], Khosroyjerdi et al. presented an ANFIS based MPPT controller with a DC-DC converter. The simulation results highlighted the benefits of determining duty cycle and reference voltage as output membership functions of the control system without using the voltage and current sensors. The presented method has the following disadvantages:

- Several energy management strategies designs are based on the small-signal model. that's mean cannot guarantee global stability.
- Many existing models suffer from incomplete plant dynamics because they ignore the inner controllers' impact on the control, thus affecting both the performance and stability of converters.

To overcome the aforementioned difficulties, this paper proposes a new, home energy management for an islanded and grid-connected microgrids. we can summarize the main advantages of the proposed method as follows:

- To the best of the authors' knowledge, this paper is the first to propose a home energy management control for both frequency and voltage restoration of a grid-connected microgrid and islanded microgrid based on consideration of a complete nonlinear system model, irrespective of parametric disturbances and uncertainties.
- In the case of frequency restoration, the distributed consensus-based control demonstrates the accuracy of power-sharing.
- In this paper, a new approach is proposed to design the ANFIS based maximum power point tracking for the photovoltaic system.

### 3. Proposed System Description

Figure 1 illustrates the overall configuration of the proposed system which includes a photovoltaic system with maximum power point tracking control and inverter control, battery, and control. The system incorporates a battery source as a backup unit for supplying power during emergency conditions to critical loads and also for maintaining the voltage and frequency in the microgrid. The battery is usually

placed parallel to the photovoltaic system. The batteries either absorb or injects real power via a converter.

The converter operates in boost mode when the battery feeds the power into a grid or load and operates in buck mode when the battery draws power from the photovoltaic array. The battery either injects or absorbs real power via a converter. The batteries are usually placed parallel to the photovoltaic system. The converter operates in boost mode when the batteries feed the power to load or grid and operates in buck mode when the batteries draw power from the photovoltaic array. The lead-acid batteries are commonly selected for photovoltaic applications.

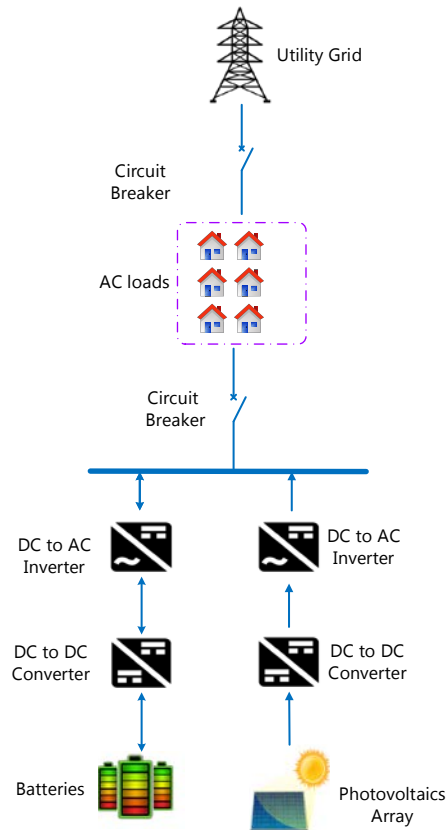


Fig. 1. The proposed system structure.

#### 4. Adaptive Neuro-Fuzzy Inference System Architecture

It is a process for mapping of given data set from multi inputs or a single input to a single output which is achieved by the fuzzy logic and the artificial neuro networks. Using given input-output data sets, ANFIS constructs a Fuzzy Inference System (FIS) whose fuzzy membership function parameters are adjusted using hybrid learning method includes back propagation and least square algorithms [17, 18].

For simplicity, it is assumed that the fuzzy inference system has two inputs  $x$  and  $y$  and one output  $z$ . The common rules set with fuzzy if then rules are given as [19, 20]:

Rule 1: If  $x$  is  $A_1$  and  $y$  is  $B_1$ , then  $f_1 = p_1x + q_1y + r_1$

Rule 1: If  $x$  is  $A_2$  and  $y$  is  $B_2$ , then  $f_2 = p_2x + q_2y + r_2$

The reasoning mechanism for this model is shown in Fig. 2(a). The equivalent ANFIS architecture is shown in Fig. 2(b), where nodes of the same layer have similar functions, as described next. (Here, the output of the  $i$ th node in layer  $l$  is denoted as  $O_{l,i}$ ).

**Layer 1.** Every node  $i$  in this layer is an adaptive node with a node function

$$O_{1,i} = \begin{cases} \mu_{A_i}(x) & \text{for } i = 1,2 \\ \mu_{B_{i-2}}(y) & \text{for } i = 3,4 \end{cases} \quad (1)$$

where  $y$  (or  $x$ ) is the input to node  $i$  and  $A_i$  (or  $B_{i-2}$ ) is a linguistic value (such as "hot" or "cold") associated with this node. In other words,  $O_{1,i}$  is the membership grade of a fuzzy set  $A$  ( $A_1, A_2, B_1$  or  $B_2$ ) and it specifies the degree to which the given input  $x$  (or  $y$ ) satisfies the quantifier  $A$ . The membership function for  $A$  can be any appropriate parameterized membership function, such as the generalized triangle function:

$$\mu_{A_i}(x) = \begin{cases} 0 & x \leq a_i \\ \frac{x-a_i}{b_i-a_i} & a_i \leq x \leq b_i \\ \frac{c_i-x}{c_i-b_i} & b_i \leq x \leq c_i \\ 0 & x \geq c_i \end{cases} \quad (2)$$

where  $(a_i, b_i, c_i)$  are the parameter sets. The parameters  $a_i$  and  $c_i$  locate the feet of the triangle and the parameter  $b_i$  locates the peak of the triangle. As the values of these parameters change, the triangle-shaped function varies accordingly, thus exhibiting various forms of membership function for fuzzy set  $A$ . Parameters in this layer are referred to as premise parameters and they will be adaptive during learning phase.

**Layer 2.** Every node in this layer is a fixed node labelled  $\Pi$ , whose output is the product of all the incoming signals

$$O_{2,i} = w_i = \mu_{A_i}(x) \times \mu_{B_i}(x), \quad i = 1,2 \quad (3)$$

Each node output represents the firing strength of a rule. In general, any other T-norm operators that perform fuzzy AND can be used as the node function in this layer.

**Layer 3.** Every node in this layer is a fixed node labelled  $N$ . The  $i$ th node calculates the ratio of the  $i$ th rule's firing strength to the sum of all rules' firing strengths:

$$O_{3,i} = \bar{w}_i = \frac{w_i}{w_1+w_2}, \quad \text{for } i = 1,2 \quad (4)$$

Outputs of this layer are called normalized firing strengths.

**Layer 4.** Every node  $i$  in this layer is an adaptive node with a node function:

$$O_{3,i} = \bar{w}_i f_i = \bar{w}_i(p_i x + q_i y + r_i) \quad i = 1,2 \quad (5)$$

where  $\bar{w}_i$  is a normalized firing strength from Layer 3 and  $\{p_i, q_i, r_i\}$  are the parameter sets of this node. Parameters in this layer are referred to as consequent parameters and they will be adaptive during learning phase.

**Layer 5.** The single node in this layer is a fixed node labelled  $\Sigma$ , which computes the overall output as the summation of all incoming signals:

$$\text{Overall output} = O_s = \sum_i \bar{w}_i f_i = \frac{\sum_i w_i f_i}{\sum_i w_i} \quad (6)$$

Thus, an adaptive network has been constructed. It is functionally equivalent to a Sugeno fuzzy model.

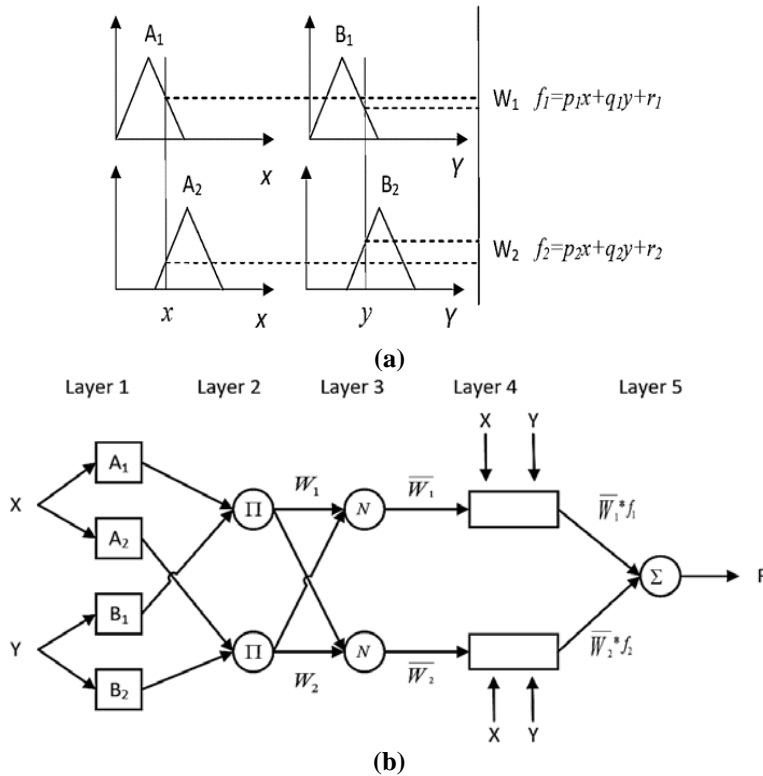


Fig. 2. (a) Two inputs first order Sugeno with two rules. (b) Equivalent typical ANFIS architecture [20].

### 5. Maximum Power Point Tracking Methods

There are many MPPT methods available in literatures which can be classified into two categories direct and indirect methods. Direct methods are based on the principle that the slope of the PV module power-voltage curve is positive on the left of the MPP, zero at the MPP, and negative on the right; or any alternative relationships derived from this principle. They always require only voltage and current sensors. Direct methods are Perturb and Observe method (P & O), Incremental Conductance (Inc. Cond.) method, Fuzzy Logic Control (FLC) method, and slide control method. Indirect methods are not based on the operating principle of the direct methods, where MPP estimates from irradiation, temperature, empirical data, and/or mathematical expressions of numerical approximation as well as voltage and/or current. The estimation in this method is carried out for a specific PV module while direct method is not required prior knowledge of PV module, therefore MPP tracking of the direct method is true while MPP tracking of the indirect method is quasi. Indirect methods are constant voltage method, curve fitting method, lookup table method, fractional open circuit voltage method, and fractional short circuit current method.

The proposed ANFIS-reference model method is one of the indirect methods since MPP estimates from given irradiation and temperature. In this paper, three methods which are the constant voltage method, the incremental conductance method, and the proposed ANFIS-reference model method; will be highlighted.

### 6. Constant Voltage Method Based MPPT

The constant voltage algorithm is the simplest MPPT method. The operating point of the PV module is kept near the MPP by regulating the PV module voltage and matching it to a fixed reference voltage ( $V_{ref}$ ). The  $V_{ref}$  value is set equal to the  $V_{mpp}$  of the characteristic PV module under standard conditions (1000 W/m<sup>2</sup> irradiation and 25 °C temperature). This method assumes that effects of the irradiation and temperature variations on the PV module are insignificant and that the constant reference voltage is an adequate approximation of the true MPP. Therefore, the operation is never exactly at the MPP because irradiation and temperature variations differs respect to different geographical regions.

The constant voltage method gives a simplified system and low cost to implement since it does require only one input  $V_{PV}$  as well as it is cheap. The duty cycle change of the DC/DC convertor ( $\Delta D$ ) is controlled by a controller which calculates error value ( $e$ ) as difference between  $V_{ref}$  and  $V_{PV}$ , as shown in Fig. 3 [2, 21].

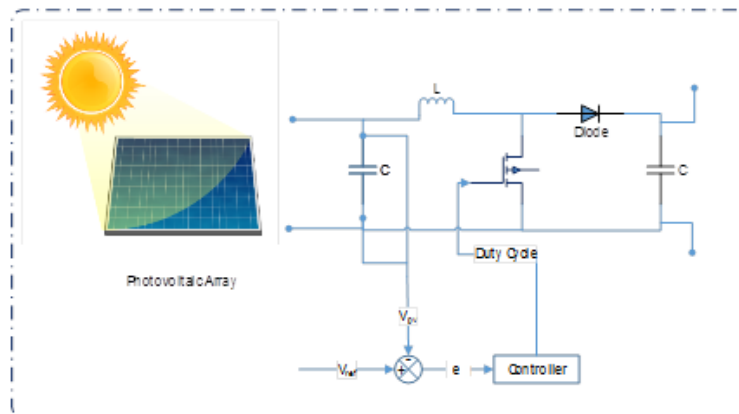


Fig. 3. Block diagram of constant voltage method based MPPT.

### 7. Incremental Conductance Method Based MPPT

The incremental conductance method is the most commonly used MPPT for PV systems. It is based on the fact that the derivative of the power of a PV module with respect to voltage is positive on the left of the MPP, zero at the MPP and negative on the right.

$$\begin{cases} \frac{dP}{dV} > 0 & \text{left of MPP} \\ \frac{dP}{dV} = 0 & \text{at PP} \\ \frac{dP}{dV} < 0 & \text{right PP} \end{cases} \quad (7)$$

Since

$$\frac{dP}{dV} = \frac{d(VI)}{dV} = I + V \frac{dI}{dV} \approx I + V \frac{\Delta I}{\Delta V} \quad (8)$$

Equation (12) can be rewritten as:

$$\begin{cases} \frac{\Delta I}{\Delta V} > 0 & \text{left of MPP} \\ \frac{\Delta I}{\Delta V} = 0 & \text{at MPP} \\ \frac{\Delta I}{\Delta V} < 0 & \text{right MPP} \end{cases} \quad (9)$$

The MPP can thus be tracked by comparing the instantaneous conductance ( $I/V$ ) to the incremental conductance ( $\Delta I/\Delta V$ ) as shown in the flow chart in Fig. 4. Therefore the sign of the quantity  $(\Delta I/\Delta V) + (I/V)$  indicates the correct direction of perturbation leading to the MPP. When MPP has been reached, the operation of PV module is maintained at this point and the perturbation stopped unless a change in  $\Delta I$  is noted. In this case, the algorithm decrements or increments the  $V_{ref}$  to track the new MPP. The perturbation step size ( $\Delta D$ ) determines how fast the MPP is tracked [22]. However, the selection of the perturbation step size is difficult because of the trade-off between fast dynamic response and steady state performance [2, 23]. It is important to observe that when the PV module is in low irradiation conditions, the constant voltage method is more effective than either the perturbation and observation method or the incremental conductance method because perturbation may be stopped since change in  $\Delta I$  is too small.

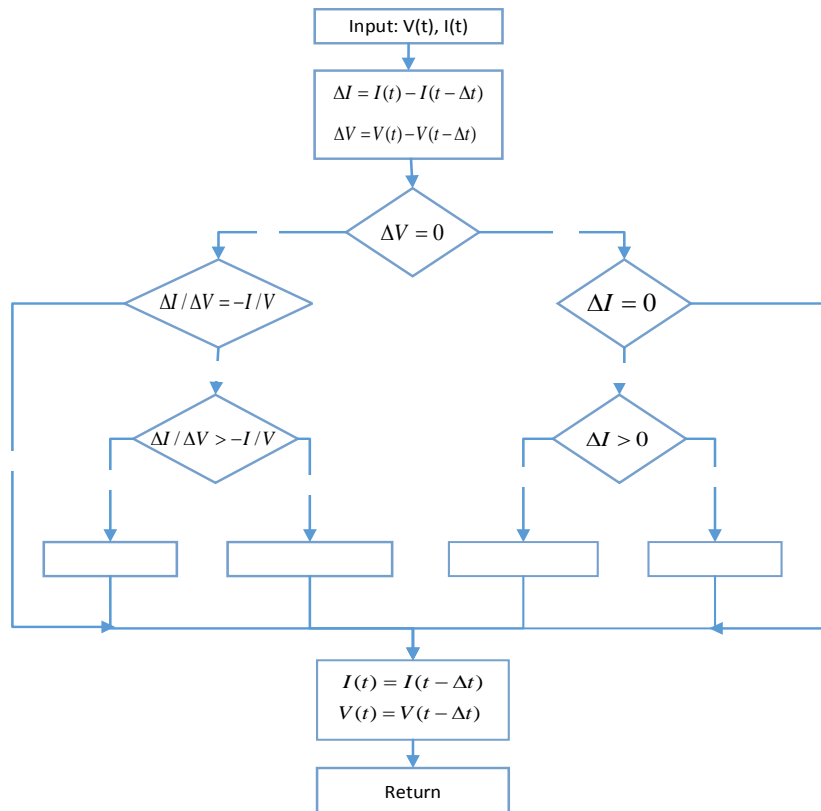


Fig. 4. Incremental conductance flow chart based MPPT.



### 8. The ANFIS-Reference Model Method Based MPPT

The new proposed controller is composed of ANFIS-reference model and current controller as shown in Fig. 5. The ANFIS is employed as reference model due to the complex nonlinear relations between the irradiation and temperature which represent input variables and  $I_{mpp}$  represents output variable. The adaptive neuro-fuzzy inference system is trained with data sets obtained from voltage- current and voltage- power characteristic of the 6000 W photovoltaic module, to generate maximum power corresponding to the given irradiation and temperature. The current controller is employed to force the PV module current ( $I_{pv}$ ) tracks  $I_{mpp}$  by changing duty cycle of the buck converter. The error ( $e$ ) is difference between  $I_{mpp}$  which is as set point and  $I_{pv}$ . The error is given to current controller to control output signal which changes duty cycle of the buck converter [18].

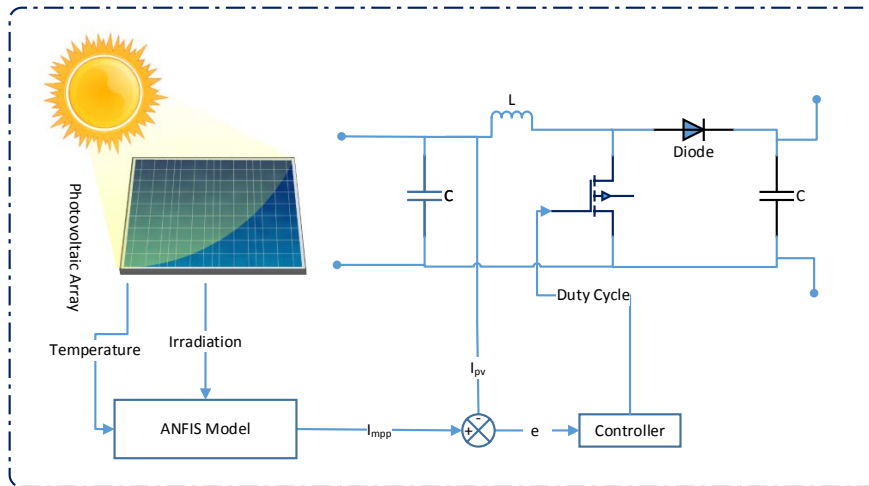
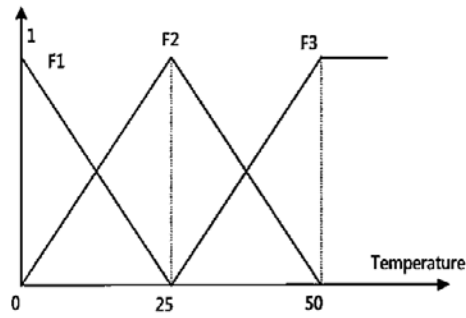


Fig. 5. The diagram of the proposed adaptive neuro-fuzzy inference system -reference model-based maximum power point tracking.

### 9. Design and Implementation of ANFIS Based MPPT

The adaptive neuro-fuzzy inference system design is based on Sugino model. It has two input variables which are: the temperature ( $T$ ), the irradiation ( $G$ ), and one output ( $I_{mpp}$ ) is fed to the current controller. It has been chosen three triangle membership functions for each input. Figures 6 and 7 illustrate the fuzzy set of the temperature and the irradiation respectively.

If the output of ANFIS is considered as a voltage signal ( $V_{mpp}$ ), but in this case, the root meaning of the square error will be 11.71%, while if the output of ANFIS is considered as the current signal ( $I_{mpp}$ ), the root mean of the square error will be 1.44%. Therefore, the output of ANFIS has been selected as  $I_{mpp}$  because it is better than the selection of the output of  $V_{mpp}$  as the output of ANFIS for the same number and types of membership functions. After setting data sets, the controller has been trained for 200 epochs by the Matlab toolbox. Figure 8 illustrates the surface view of the fuzzy rules created by ANFIS.



**Fig. 6. Fuzzy set of temperatures.**

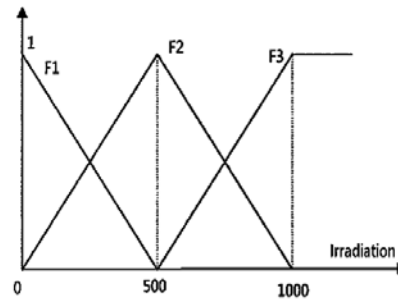


**Fig. 7. The fuzzy set of irradiation.**

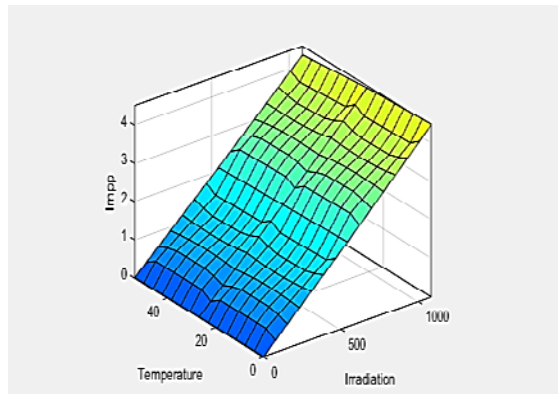


**Fig. 8. The surface view created by ANFIS.**

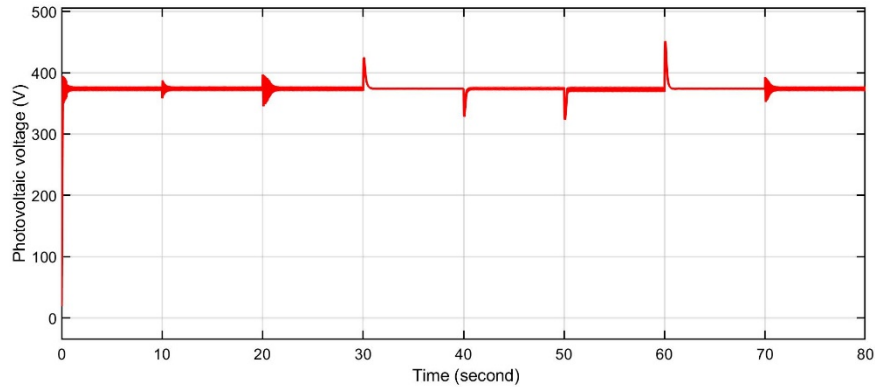
## 10. Home Energy Management System

In the mode of islanded, the battery is used as a back-up source of power in the case where photovoltaic generated power is lower than consumer power demand. In this mode, when the photovoltaic source produces more power than that of connected loads, then the excess power is stored in the battery. The stored energy in a battery is used whenever the power demand of consumption exceeds the actual photovoltaic power generation. In the mode of grid-connected operation, the battery is enabled to charge from utility power and photovoltaic. In this operating mode, the generated power from photovoltaic is delivered to the batteries at a constant rate. At the time of beginning, photovoltaic array produces lower power from which the battery can't charge. During this condition, grid power is taken by the inverter as supplementary energy. As soon as the battery charge power reduces, the inverter begins to supply power into the grid. Once the battery gets fully charged, all the generated power from photovoltaic is delivered to the grid.

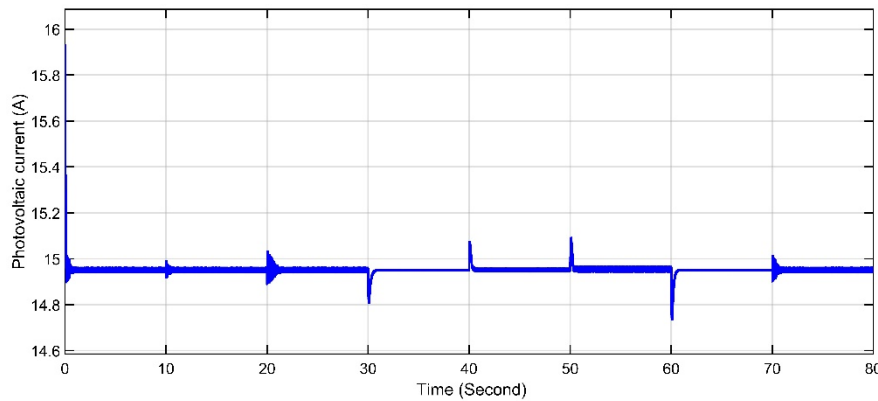
## 11. Simulation Results

To show the effectiveness of the proposed control method using ANFIS, the hybrid AC/DC microgrid systems are simulated under islanded and grid-connected operations. At first, the batteries are assumed to be in fully charged condition and loads are yet to be connected to the system. The power grid is connected to domestic

from the distribution transformer. The surplus power from the home energy management system is fed into the power grid. Also, it can supply power to the home energy management system in the case of a shortage of power generation in the photovoltaic system. This transfer of power between the home energy management system and the power grid takes place with the help of a bidirectional DC to AC inverter. The photovoltaic is allowed to operate at its standard test condition with an operating 1000 W/m<sup>2</sup> Irradiation and 25 °C temperature. The simulation is carried out for 80 seconds. The total power generated by the photovoltaic array is maintained constant at 6 kW by the MPPT controller. The output current and voltage of the photovoltaic are shown in Fig. 9, where photovoltaic voltage  $V_{PV}$  is always maintained at its maximum value.



(a)

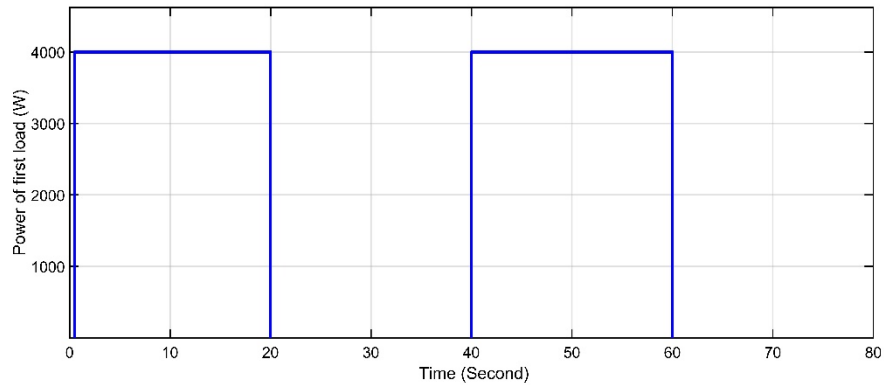


(b)

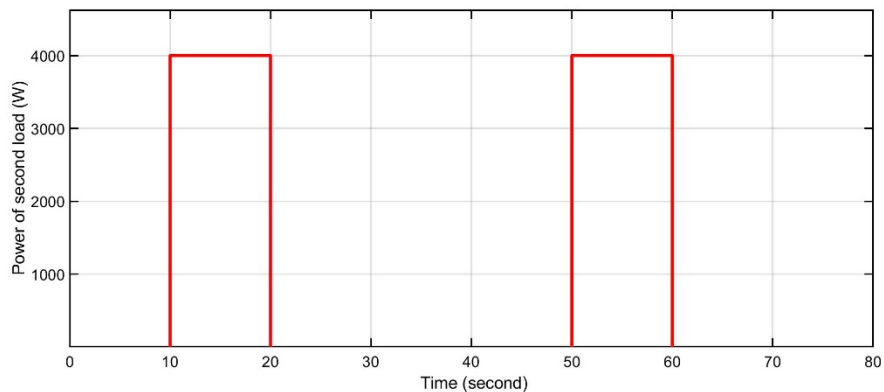
**Fig. 9. Photovoltaic array voltage and current at MPPT.**

The load on the system is enabled at the specified intervals. In this study, two PQ loads of each having a rating of 4 kW real power and 100 AVR of reactive power is connected to the home energy management system.

Consider the operation grid-connected mode, where the load 1 of 4 kW is connected at time  $t=0.75$  second. The load consumes more than half of the power generated by the photovoltaic array and remaining power is returned to the power grid. At time  $t=10$  second, the load 2 is connected. Now, the total load on the system is 8000 W which is more than the power generated by the photovoltaic system. Hence, the shortage of power is supplied to the consumer by the utility power. Therefore, the grid will help to balance the power demand of consumers along with the photovoltaic system. The load of residential at different times is shown in Fig. 10



(a)



(b)

**Fig. 10. Load variation at home for many time,  
(a) First load, and (b) Second load**

Now in order to test the behaviour of the proposed system in transition condition, the grid is now disabled at time  $t=30$  second. Now the microgrid operates in an island mode of operation. The system response to load variation from 4 kW to 8 kW. In this mode, the photovoltaic system is allowed to generate its maximum power of 6 kW. Batteries come into picture in the islanded mode of operation. The battery will supply the complementary power required to meet consumer power demand. The output of inverter decreases or increases based on the requirement of load power, while the DC-link voltage is kept constant. Maximum power point

tracking controller provides the reference value for DC-link voltage and is maintained constant by the battery DC/DC converter by delivering or absorbing the adequate power. Again, the load 1 and load 2 of capacity 4 kW each is connected to the home energy management system at time  $t=40$  second and  $t=50$  second respectively. During the connection of load 1, the photovoltaic array supplies the required power as the power demand is below the photovoltaic generated power. When load 2 is connected to the home energy management system, the total load becomes 8 kW is higher than the photovoltaic generated power. The battery power is enabled to supply this difference of power to make power balance. The following Fig. 11 and 12 illustrate the various parameters home energy management system in the grid-connected and islanded mode of operation.

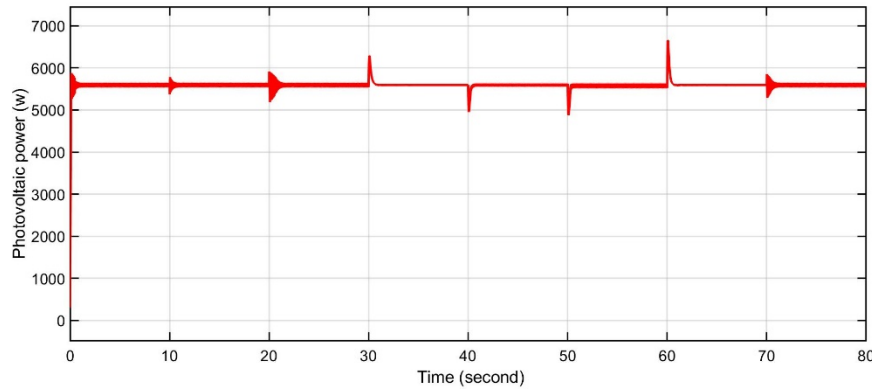


Fig. 11. Photovoltaic response of the neuro-fuzzy controller-based maximum power point.

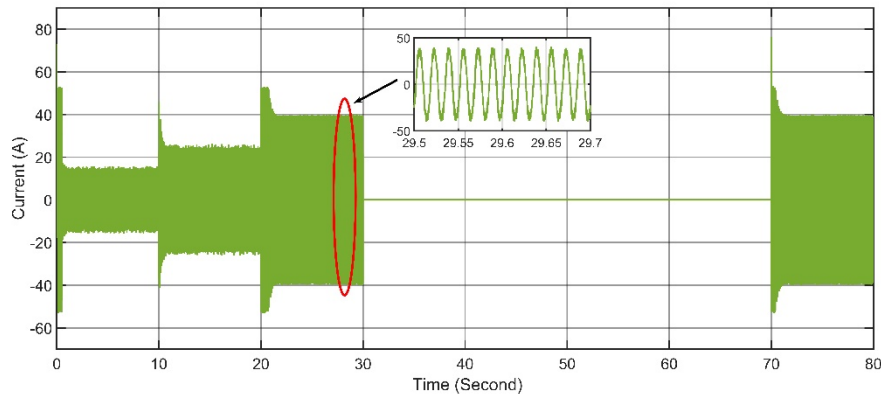
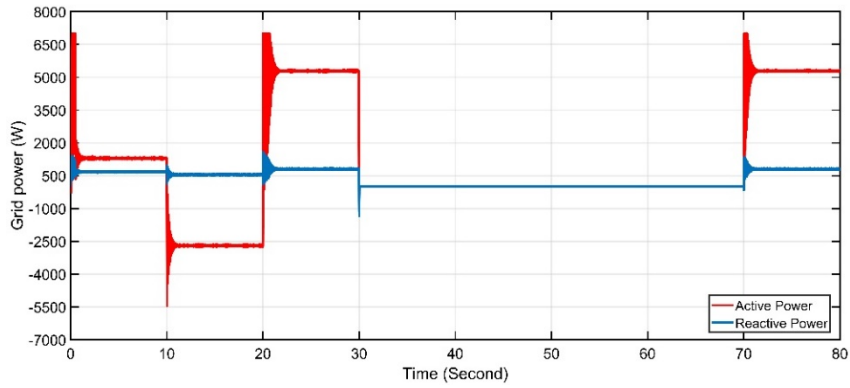


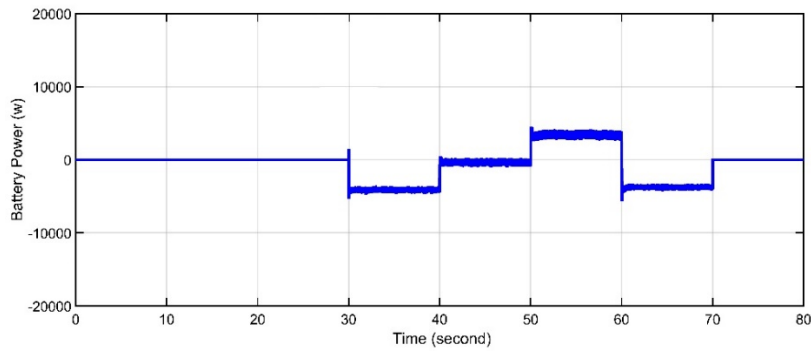
Fig. 12. Current contributed via the grid for island and grid modes.

Figure 11 shows the power generated by the photovoltaic array. The total power generated almost maintained constant throughout the simulation at 6 kW. It is clear that for the time interval from  $t=0$  second to 30 seconds, the system operated in grid-connected mode drawing power from both grid and photovoltaic systems. From time interval  $t=30$  second to 70 seconds, the grid is disabled and now the system is operated in islanded mode feeding power to loads from both photovoltaic system and battery. Figure 12 shows the current drawn from the utility grid. It is evident that the grid does

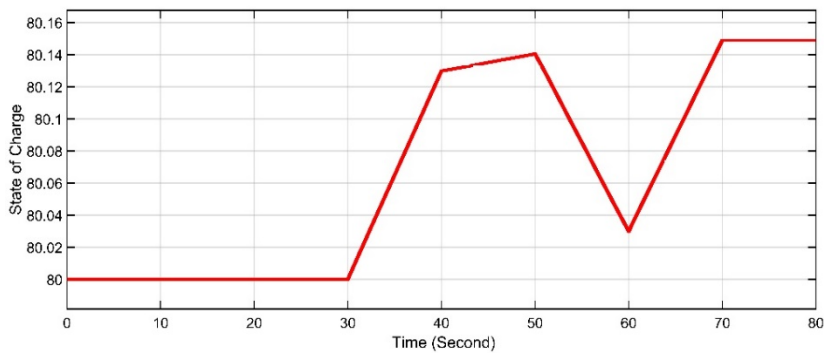
not contribute to load during the interval of time  $t=30$  to  $70$  seconds, as the grid is disabled. Figure 13 replicates the power drawn from the grid to meet the demand power of residential homes. Figure 14 shows the battery parameters current, voltage, SoC and power during island operating mode at the time of transfer from the grid to island mode, the battery starts to discharge energy into an inverter for meeting the insufficient power that is not been ably met by the photovoltaic system.



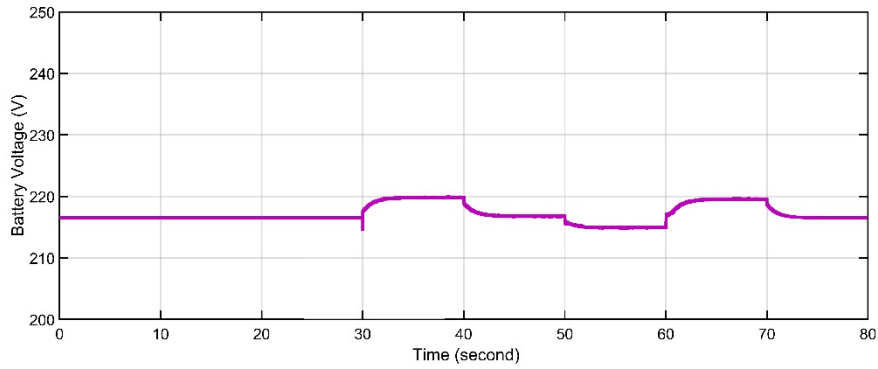
**Fig. 13. The active and reactive power of utility grid.**



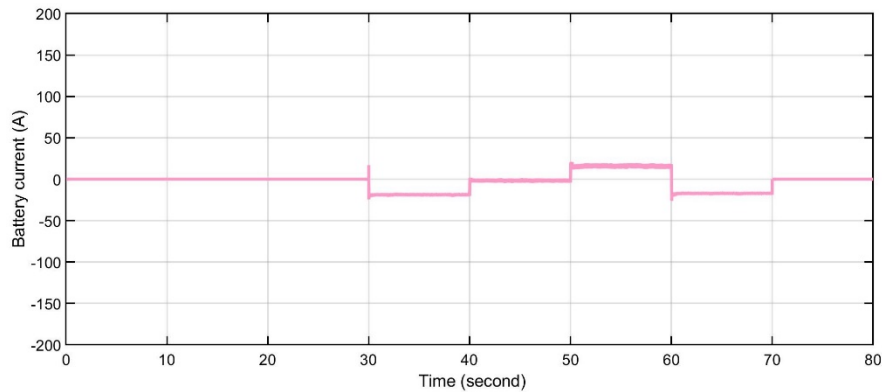
**(a)**



**(b)**



(c)



(d)

**Fig. 14. (a) Battery power, (b) State of charge of battery, (c) Battery voltage, and (d) Battery current**

### Conclusions

In this work, a novel home management system shows effectiveness in delivering uninterrupted power to the consumer through various controller designs is proposed. Also, this paper proposes an effective control strategy for a smooth transition from grid-connected to islanding mode due to unintentional islanding. The simulation results reveal that the incremental conductance and the ANFIS-reference model methods collect more daily energy than the constant voltage method when ambient temperature is high. However, the irradiation and load variations tests show that the incremental conductance method is less dynamic response, stable and more oscillatory about the MPP than the two other methods since it has small fixed perturbation step size ( $\Delta D$ ) and is sensitive to a high frequency noise. Therefore, it may tend to drift away from the MPP. Hence, the proposed method is more efficient than the two other methods. The outcomes suggested that the alternating integration of solar energy sources and batteries in the microgrid should be devised carefully in individual operation. The recommended control schemes provide exceptional performance under various operating conditions. Batteries improve the system

reliability since they store additional renewable energy when the demand is low and supply energy when the demand is high. As future works, the following points are suggestions; 1) implementing the presented strategy on a real network and comparing the results, 2) investigating the effects of other uncertain parameters such as fuel cost on the microgrid planning.

## References

1. Naji Alhasnawi, B.; Jasim, B.H.; Issa, W.; Esteban, M.D. (2020). A novel cooperative controller for inverters of smart hybrid ac/dc microgrids. *Applied Sciences*, 10(17), 1-24.
2. Senthil Kumr, M.; and Rajakumr, P. (2017). Modelling and implementation of home energy management system for renewable energy based hybrid system to residential application. *International Journal of Industrial Electronics and Electrical Engineering*, 5(9), 43-51.
3. Bidram, A.; and Davoudi, A. (2012). The hierarchical structure of microgrids control system. *IEEE Transactions on Smart Grid*, 3(4), 1963-1976.
4. Issa, W. R.; Ahmad H. El Khateb; Mohammad, A. Abusara.; and Tapas K. Mallick. (2018). Control strategy for uninterrupted microgrid mode transfer during unintentional islanding scenarios. *IEEE Transactions on Industrial Electronics*, 65(6), 4831-4839.
5. Issa, W.; Sharkh, S.; and Abusara, M. (2019). Hybrid generators-based ac microgrid performance assessment in island mode. *Institutions Electric Technology: Power Electronics*, 12(8), 1973-1980.
6. Al Badwawi, R.; Issa, W.R.; Mallick, T.P.; and Abusara, M. (2019). Supervisory control for power management of an islanded ac microgrid using a frequency signalling-based fuzzy logic controller. *IEEE Transactions on Sustainable Energy*, 10(1), 94-104.
7. Al-naemi, F.; Issa, W.; Asmaiel, R.; and Hall, J. (2018). Design and modelling of permanent magnet fault current limiter for electrical power applications. *2018 53rd International Universities Power Engineering Conference (UPEC)*, Glasgow, UK. 4-7.
8. Issa, W.; Sharkh, S.M.; Albadwawi, R.; Abusara, M.; and Mallick, T.K. (2017). DC link voltage control during sudden load changes in AC microgrid. *2017 IEEE 26th International Symposium on Industrial Electronics (ISIE)*, Edinburgh, UK. 19-21.
9. Issa, W.R.; Abusara, M.A.; Suleiman M. Sharkh. (2015). Control of transient power during unintentional islanding of microgrids. *IEEE Transactions on Power Electronics*, 30(8), 4573-4584.
10. Issa, W.; Abusara, M.A.; Sharkh, S.M.; and Mallick, T. (2015). A small signal model of an inverter-based microgrid including DC link voltages. *17th European Conference on Power Electronics and Applications (EPE'15 ECCE-Europe)*, Geneva, Switzerland. 8-10.
11. Issa, W.R.M. (2015). *Improved Control Strategies for Droop-Controlled Inverter-Based Microgrid*, Ph.D. Thesis, University of Exeter, Exeter, United Kingdom.
12. Lujano, J. M.; Monteiro, C.; Dufo-Lopez, R.; and Bernal-Agustin, J. L. (2012). Optimum load management strategy for wind/diesel/battery hybrid power systems. *Journal of Renewable Energy*, 4(44), 288-295.



13. Kalika, S.; Rajaji, L.; and Gupta, S. (2013). Neuro-fuzzy based peak power point tracking for solar photovoltaic system, *International Journal of Computer Applications*, 64(13), 11-16.
14. Kharb, R.K.; Ansari, M.F.; and Shimi, S.L. (2014). Design and implementation of ANFIS based MPPT scheme with open loop boost converter for solar PV module, *International Journal of Advanced Research in Electrical, Electronics and Instrumentation Engineering (IJAREEIE)*, 4(89). 6517-6524.
15. Mahdavi, M.; Li, L.; Zhu, J.; and Mekhilef, S. (2015). An adaptive neuro fuzzy controller for maximum power point tracking of photovoltaic systems, *IEEE Proceedings of the First Asian Pacific Conference on power*, Osaka, Japan. 1-6.
16. Khosrojerdi, F.; Taheri, S.; and Cretu, A.M. (2016). An adaptive neuro-fuzzy inference system based MPPT controller for photovoltaic arrays. *IEEE Electrical Power and Energy Conference (EPEC)*, 1-6.
17. Mohammed, S.S.; Devaraj, D.; Ahamed, T.P.I. (2016). Maximum power point tracking system for stand-alone solar PV power system using adaptive neuro-fuzzy inference system, *IEEE, Biennial International Conference on Power and Energy Systems: Towards Sustainable Energy (PESTSE)*, 1-4.
18. Aldair, A.A.; Obed, A.A.; and Halihal, A.F. (2018). Design and implementation of ANFIS-reference model controller based MPPT using FPGA for photovoltaic system. *Renewable and Sustainable Energy Reviews*, 82(4), 2202-2217.
19. Hakim, S.J.S.; and Razak, H.A. (2012). Damage identification using experimental modal analysis and Adaptive Neuro-Fuzzy Interface System (ANFIS). *Conference Proceedings of the Society for Experimental Mechanics Series*, 30(5), 399-404.
20. Ali Fadhil Halihal. (2016). Design and Implementation of Neuro-Fuzzy Controller Using FPGA for Sun Tracking System. Iraq, Basrah: *Master Thesis, Electrical Engineering Department*, University of Basrah.
21. Naji Alhasnawi, B.; Jasim, B.H.; Esteban, M.D. (2020). A New Robust Energy Management and Control Strategy for a Hybrid Microgrid System Based on Green Energy. *Sustainability*, 12(14), 5724.
22. ESRAM, T.; and Chapman P. (2007). Comparison of photovoltaic array maximum power point tracking techniques. *IEEE Transactions on Energy Conversion*; 22(2):439-49.
23. Weidong, X. (2003). A modified adaptive hill climbing maximum power point tracking (MPPT) control method for photovoltaic power systems. *Master Thesis*, University of British Columbia.